Received: 26 December 2019 | Revised: 3 April 2020 | Accepted: 10 May 2020

DOI: 10.1002/ajpa.24082



BRIEF COMMUNICATION

American Journal of PHYSICAL ANTHROPOLOGY WILEY

# Reassessment of the TM 1517 odonto-postcranial assemblage from Kromdraai B, South Africa, and the maturational pattern of *Paranthropus robustus*

Marine Cazenave[1,2] | Christopher Dean[3,4] | Clément Zanolli[5] | Anna C. Oettlé[2,6] | Jakobus Hoffman[7] | Mirriam Tawane[8] | Francis Thackeray[9] | Roberto Macchiarelli[10,11]

[1]Skeletal Biology Research Centre, School of Anthropology and Conservation, University of Kent, Canterbury, UK

[2]Department of Anatomy and Histology, Sefako Makgatho Health Sciences University, Ga-Rankuwa, Pretoria, South Africa

[3]Department of Earth Sciences, Natural History Museum, London, UK

[4]Department of Cell and Developmental Biology, University College London, London, UK

[5]UMR 5199 CNRS, Université de Bordeaux, Bordeaux, France

[6]Department of Anatomy, University of Pretoria, Pretoria, South Africa

[7]South African Nuclear Energy Corporation SOC, Ltd., Pelindaba, South Africa

[8]Ditsong National Museum of Natural History, Pretoria, South Africa

[9]Evolutionary Studies Institute and School of Geosciences, University of the Witwatersrand, Johannesburg, South Africa

[10]UMR 7194 CNRS, Muséum national d'Histoire naturelle, Musée de l'Homme, Paris, France

[11]Unité de Formation Géosciences, Université de Poitiers, Poitiers, France

**Correspondence**
Marine Cazenave, Department of Anatomy and Histology, Sefako Makgatho Health Sciences University, Ga-Rankuwa, Pretoria, South Africa.
Email: marine.cazenave4@gmail.com

**Funding information**
Erasmus Mundus programme, Bakeng se Afrika; European Commission (EACEA); AESOP and AESOP + consortia; National Equipment Program (NEP) of the DST-NRF, Grant/Award Number: # UID23456; NRF Incentive Grant (Associated with the NRF Rated Scientist A. C. Oettlé)

## Abstract

**Objectives:** The Pleistocene taxon *Paranthropus robustus* was established in 1938 following the discovery at Kromdraai B, South Africa, of the partial cranium TM 1517a and associated mandible TM 1517b. Shortly thereafter, a distal humerus (TM 1517g), a proximal ulna (TM 1517e), and a distal hallucial phalanx (TM 1517k) were collected nearby at the site, and were considered to be associated with the holotype. TM 1517a-b represents an immature individual; however, no analysis of the potentially associated postcranial elements has investigated the presence of any endostructural remnant of recent epiphyseal closure. This study aims at tentatively detecting such traces in the three postcranial specimens from Kromdraai B.

**Materials and Methods:** By using μXCT techniques, we assessed the developmental stage of the TM 1517b's C-M3 roots and investigated the inner structure of TM 1517g, TM 1517e, and TM 1517k.

**Results:** The M2 shows incompletely closed root apices and the M3 a half-completed root formation stage. The distal humerus was likely completely fused, while the

proximal ulna and the distal hallucial phalanx preserve endosteal traces of the diaphyseo-epiphyseal fusion process.

**Discussion:** In the hominin fossil record, there are few unambiguously associated craniodental and postcranial remains sampling immature individuals, an essential condition for assessing the taxon-specific maturational patterns. Our findings corroborate the original association of the craniodental and postcranial remains representing the *P. robustus* type specimen. As with other Plio-Pleistocene hominins, the odonto-postcranial maturational pattern of TM 1517 more closely fits an African great ape rather than the extant human pattern.

**KEYWORDS**

odonto-postcranial maturation, *P. robustus*, TM 1517, X-ray microtomography

## 1 | INTRODUCTION

The holotype of the fossil hominin taxon *Paranthropus robustus* consists of the left half of a calvaria (TM 1517a) and the associated right mandibular corpus (TM 1517b) both bearing teeth, and of seven isolated teeth (a LLP3, a LLP4, and the series URP3-M3 labeled as TM 1517c). This assemblage was discovered by Robert Broom and Gert Terblanche in 1938 in an outcrop of bone breccia at the cave site of Kromdraai B, in Gauteng, South Africa (Broom, 1938a). A few weeks later, in the same matrix and near the block including the cranial remains, Broom identified postcranial elements representing the distal end of a right humerus (TM 1517g), the partial proximal end of a right ulna (TM 1517e), and a toe bone (TM 1517k). The remains were attributed to the same young individual (Broom, 1938b, 1942) and it has been suggested that the distal humerus and the proximal ulna fit in size and anatomically (Braga & Thackeray, 2016; Skinner, Kivell, Potze, & Hublin, 2013; Thackeray, De Ruiter, Berger, & Van Der Merwe, 2001), which supports Broom's original observations. Unfortunately, the exact location where the cranial and postcranial elements forming the TM 1517 assemblage were collected in 1938 were not recorded (Thackeray, McBride, Segonyane, & Franklyn, 2003).

While the holotype certainly represents an immature individual (Braga & Thackeray, 2016; Broom, 1938b, 1942; Skinner et al., 2013; Skinner & Sperber, 1982; Thackeray et al., 2001) since their early description, no analysis of the TM 1517's postcranial elements has investigated the inner presence of any remnant of epiphyseal fusion.

Using imaging techniques applied to an X-ray microtomographic (μXCT) record, we performed a study aimed at tentatively detecting any trace of a recent, or incomplete epiphyseal closure characterizing the inner structure of the distal humerus TM 1517g, the proximal ulna TM 1517e and the distal hallucial phalanx TM 1517k. Such evidence of immaturity would corroborate the individual association of the craniodental and postcranial elements forming the TM 1517 assemblage and, importantly, would provide the first evidence of odonto-postcranial maturational pattern in *P. robustus*. Based on previous studies of Plio-Pleistocene immature hominin individuals represented by unambiguously associated dental and postcranial remains (Alemseged et al., 2006; Bolter, Elliott, Hawks, & Berger, 2020; Cameron, Bogin, Bolter, & Berger, 2017; Cofran & Walker, 2017; Dean & Smith, 2009; Kelley & Bolter, 2013; Šešelj, 2017; Smith, 2004; Vekua et al., 2002), we expect TM 1517 to show a maturational pattern that more closely approaches the extant ape rather than the human condition (cf. Kelley & Bolter, 2013; Schwartz, 2012).

## 2 | MATERIALS AND METHODS

### 2.1 | Materials

All remains comprising the TM 1517 assemblage are housed at the Ditsong National Museum of Natural History in Pretoria.

**FIGURE 1** μXCT-based medial (upper row) and occlusal (lower) views of the right mandibular portion TM 1517b. In both views, mesial is to the left. Scale bar, 1 cm


**FIGURE 2** Anterior (upper row) and posterior (lower row) views of the distal right humerus TM 1517g (a) and of the proximal right ulna TM 1517e (b), and dorsal (upper row) and plantar (lower row) views of the distal hallucial phalanx TM 1517k (c). Scale bar, 1 cm

Besides the radiographically-based dental maturational pattern assessed by Skinner and Sperber (1982), no other study has detailed the TM 1517 root formation stages of each tooth element. We used a μXCT-based 3D model of the right mandibular portion TM 1517b (Broom, 1938b; Kaszycka, 2001; Skinner & Sperber, 1982) to assess the radicular developmental stage of its six preserved tooth elements, from the canine (LRC) to the third molar (LRM3) (Figure 1). Accessorily, we also considered the evidence provided by the P3-M2 roots preserved in the left maxilla of TM 1517a.

The postcranial specimens represent: the incomplete (56.7 mm long) but well-preserved right distal humeral end TM 1517g (Figure 2a) reported by Broom (1938b) and later in more detail by Straus (1948); the right proximal ulnar fragment TM 1517e (Figure 2b), originally reported by Broom (1938b) and then extensively described by Broom and Schepers (1946); and the distal left phalanx of the hallux TM 1517k (Broom, 1942; Day & Thornton, 1986) (Figure 2c).

For comparative purposes, besides the classical reference sources illustrating the maturational stages of diaphyseo-epiphyseal fusion in extant humans (rev. in Cunningham, Scheuer, & Black, 2016), we used a skeletal sample of subadult individuals of known sex, age at death and population origin selected from the R. A. Dart Collection stored at the University of the Witwatersrand, Johannesburg (Table S1). For each anatomical element, and tentatively for each sex, we selected a set of specimens documenting different stages of the maturational process as expressed at the outer surface.

## 2.2 | Methods

We used the μXCT record of the right mandibular corpus TM 1517b. The scan was originally performed by J. Braga (University of Toulouse) and kindly made available by the curator of the Ditsong National Museum of Natural History, Pretoria (M. T.). The specimen was scanned at the microfocus X-ray tomography facility (MIXRAD) of the South African Nuclear Energy Corporation SOC, Ltd. (Necsa), Pelindaba. The final volume was reconstructed with an isotropic voxel size of 61 μm. To virtually extract the six elements forming the RLC-RLM3 tooth row, a semiautomatic threshold-based segmentation with manual corrections has been carried out by using Avizo v.8.0.0 (Visualization Sciences Group, Inc., https://www.fei.com/software/amira-avizo/). Once reconstructed in 3D, the degree of radicular development of each tooth element was evaluated using the scoring system described by Moorrees, Fanning, and Hunt Jr. (1963). Given the lower quality of the signal and poorer preservation of the

preserved teeth, uniquely for control, we also used the microtomographic record of the left maxilla of TM 1517a to score the developmental stage of its preserved P3-M2 roots.

The postcranial specimens TM 1517g, TM 1517e, and TM 1517k were also scanned between 2015 and 2017 at Necsa, Pelindaba. The final volumes were reconstructed with an isotropic voxel size of 35, 23, and 8.7 μm for the distal humerus, the proximal ulna and the distal hallucial phalanx, respectively.

All selected specimens from the R. A. Dart Collection were scanned in 2017 at Necsa at resolutions ranging from 12 to 77 μm isotropic voxel size. The microtomographic record of this subadult assemblage was used as a direct comparative source to verify the degree of congruence in the expression of the diaphyseo-epiphyseal fusion process between the periosteal and the endosteal surfaces according to three maturational stages ad hoc defined for the purposes of the present study: "fusion in progress," shown by the presence of variably expressed but still distinct traces of epiphyseal fusion; "recently achieved fusion," indicated by the presence of very faint and discontinuous remnants of the diaphyseal-epiphyseal suture line; and "complete fusion," with no suture line remnant detectable externally and/or internally (Figure 3, Table S1). In the distal humerus, fusion begins posteriorly, leaving a line open above the capitulum, lateral trochlea and proximal lateral epicondyle, the medial epicondyle being the last to solder to the shaft (Cunningham et al., 2016). The fusion of the proximal epiphysis of the ulna starts at the lateral side of the articular surface and then proceeds posteriorly and medially, the posteroinferior surface of the olecranon being always the last part to fuse (Cunningham et al., 2016).

## 3 | RESULTS

### 3.1 | Dental maturational sequence

As revealed by the newly reconstructed microtomographic scans, the canine (LRC), the third premolar (LRP3), and the first molar (LRM1) of the mandibular portion TM 1517b show complete root apical closure (stage $A_c$ of Moorrees et al., 1963). Root length of the LRM1 is 16.6 mm for the mesial and 17.9 mm for the distal root. The fourth premolar (LRP4) shows a nearly complete closure of all four root apices (stage $A_{1/2}$-$A_c$) and the second molar (LRM2) shows incompletely closed root apices (stage $A_{1/2}$). The erupted third molar (LRM3), had already formed a high root bifurcation (similar in position to M1 and M2), and its mesial and distal root length below the cervical margin approximately equal to half the length of the M2 roots (Figure 4). This suggests M3 root formation in TM 1517b is best defined as stage $R_{1/2}$ following Moorrees et al. (1963). Root length in this M3 is 11.4 mm for the mesial and 10.3 mm for the distal root, which corresponds to 71.6 and 58% of the LRM1's values, respectively.

The TM 1517a maxilla shows a dental developmental pattern consistent with TM 1517b, the UP3, UP4 and UM1 displaying complete root apical closure ($A_c$) and the UM2 showing open apices (stage $A_{1/2}$) (Figure S1).

### 3.2 | Postcranial elements

A selected μXCT slice revealing the inner morphology of each specimen is shown in Figure 5.

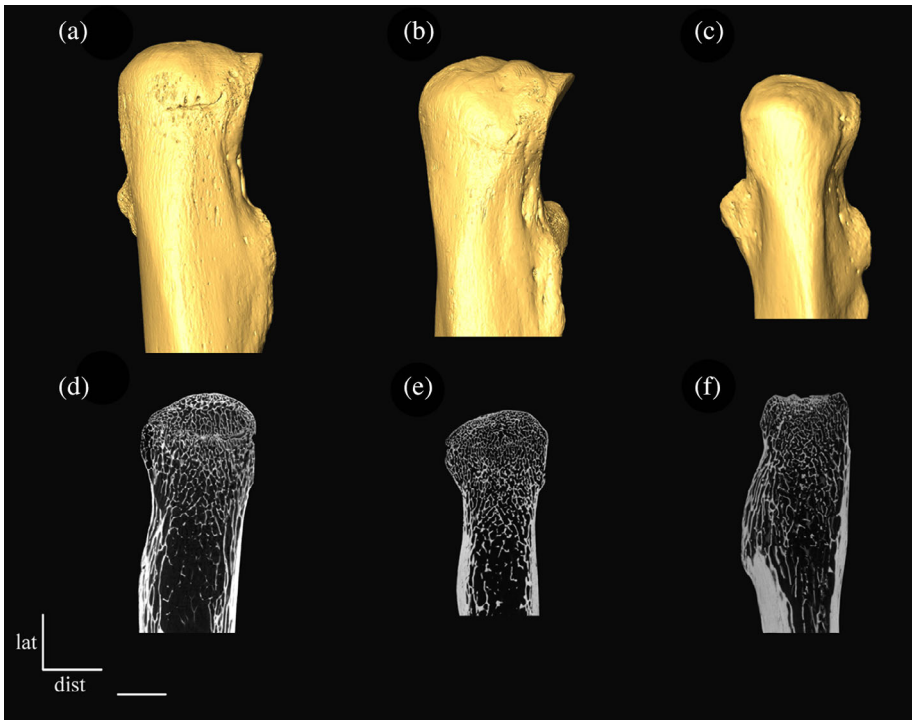


**FIGURE 3** μXCT-based posterior view of the proximal ulna of a 16 year old male (a), a 17 year old male (b) and a 14 year old female (c) individuals (upper row) and coronal slices of two 16 years old (d, e) and a 17 years old (f) male individuals (lower row) showing the following three maturational stages of diaphyseo-epiphyseal fusion expressed at the periosteal and endosteal surfaces, respectively: "fusion in progress" (a, d), "recently achieved fusion" (b, e) and "complete fusion" (c, f). Scale bar, 1 cm

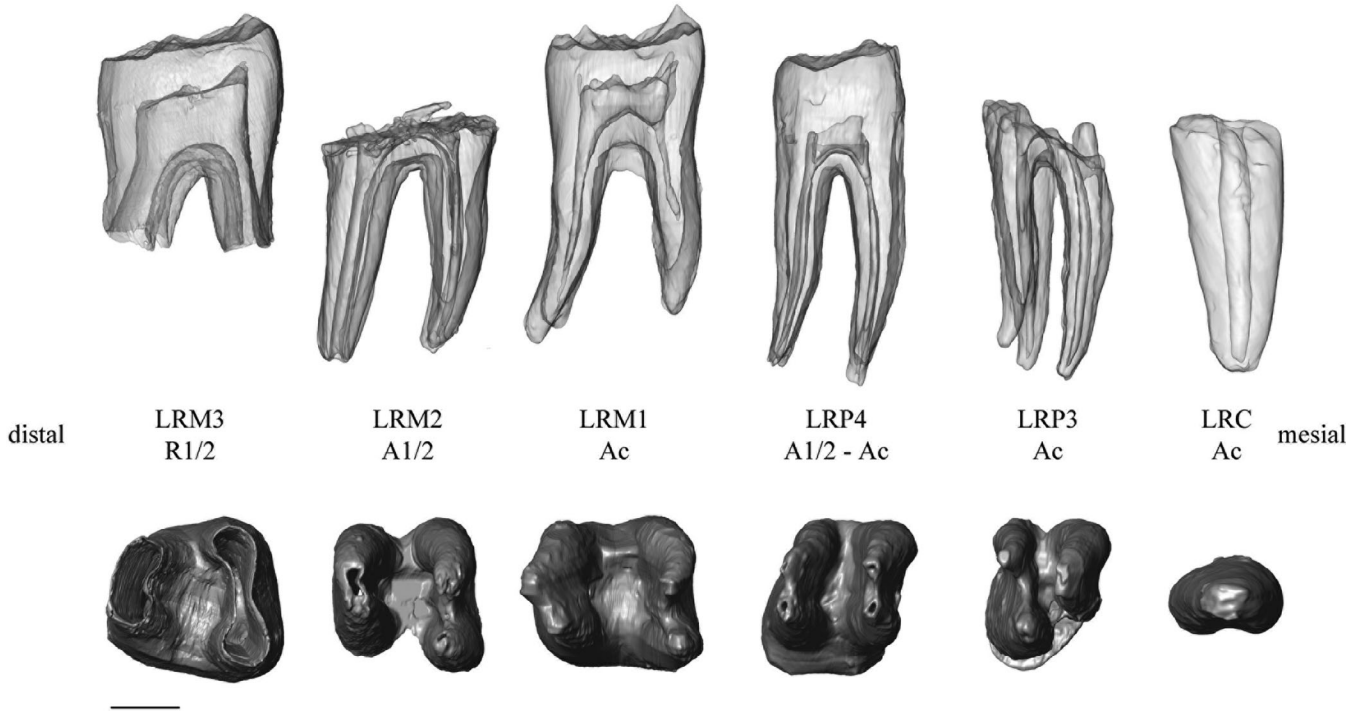


**FIGURE 4** μXCT-based virtually extracted permanent tooth elements (C to M3) of the right mandibular portion TM 1517b showing the degree of root formation (upper row) and apical closure (lower) scored following Moorrees et al. (1963). Scale bar, 5 mm

In TM 1517g, the endostructure is preserved enough to tentatively assessing its maturational status. In extant human growing individuals, variably expressed subhorizontal traces of epiphyseal fusion are found from the most lateral part of the lateral epicondyle to the most medial part of the capitulum, and from the most lateral part of the trochlea to the junction between the medial epicondyle and the trochlea (Cunningham et al., 2016). No such fusion marks are present in TM 1517g (Figure 5a). In our human reference sample, the closest fit to TM 1517g is represented by a 14 year old female (Table S1 and Figure S2).

The inner structure of the proximal ulna TM 1517e is relatively well preserved (Figure 5b). Differently from TM 1517g, in TM 1517e a remnant of epiphyseal fusion is traceable in the posteroinferior aspect of the olecranon, even if it is only faintly expressed because of the fossilization fading effect (Figure 5b). This condition should be better defined as nearly, but not fully achieved fusion, that is, as "fusion in progress." In our extant human reference sample, their closest endosteal fits are represented by a 13 year old female and a 16 year old male (Table S1 and Figure S2).

A matrix fills most of the cancellous network of the distal hallucial phalanx TM 1517k, but without completely masking its endosteal contour. Faint traces of a recently achieved epiphyseal fusion are preserved medially along the limits of the cortico-trabecular complex of the articular surface, that is, the subchondral component including the lamina and the immediately adjoining trabecular network (Cazenave et al., 2019) (Figure 5c). With respect to the extant human reference sample used in this study, its closest fit is a 14 year old female, while no male individual included in our sample documents such stage (Table S1 and Figure S2).

## 4 | DISCUSSION

Relying on high resolution microtomographic data, our 2D and 3D virtual reconstructions show that the distal humerus TM 1517g was very likely completely fused, while the proximal ulna was still in the progress of fusing, and the distal hallucial phalanx had recently achieved the stage of epiphyseal fusion. Thus, together with the anatomically-based evidence of an articulation between TM 1517g and TM 1517e, the original suggestions that the holotype TM 1517a-b and the three postcranial specimens TM 1517g, TM 1517e, and TM 1517k belong to a single immature *P. robustus* individual cannot be rejected (Broom, 1938b; Thackeray et al., 2005). In addition, the evidence that the TM 1517a maxilla and the TM 1517b mandible show a concordant root developmental pattern for the P3-M2 teeth allows us to reject the claim that "probably the cranium and mandible do not represent the same individual or even taxon" (Schwartz & Tattersall, 2005:167).

Regarding the assessment of the maturational timing and patterning in TM 1517, in Table 1 the condition of its dental and postcranial elements is compared to the age range estimates for the corresponding stages in extant humans and African great apes.

The sequence, or pattern, of LM2/LM3 development observed in TM 1517 is infrequent among recent human populations, but it certainly occurs in great apes (Choi & Kim, 1991; Dean & Wood, 2003) (Supporting Information 1). This is also concordant with previous analyses of the M1 of the likely *P. robustus* specimen SK 63 from Swartkrans, which shows the emergence and root extension rates in accordance with those known for modern great apes and fall beyond the known ranges for modern humans

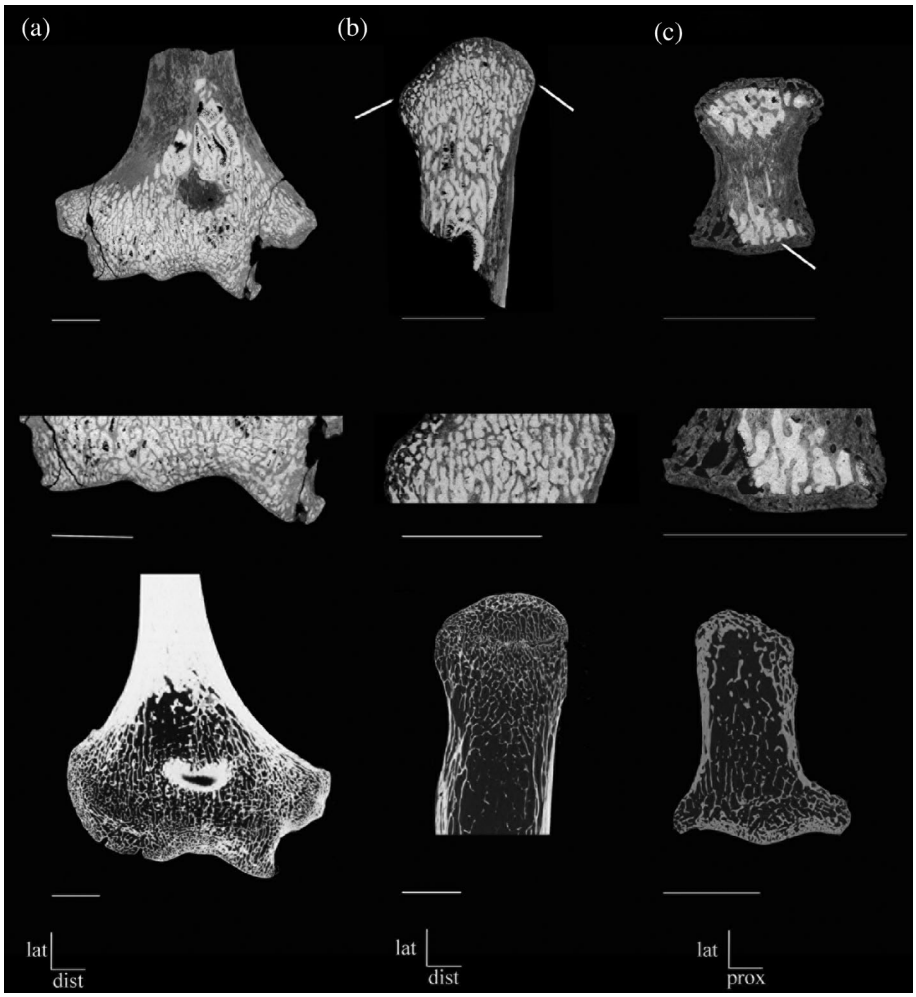


**FIGURE 5** μXCT-based (a) coronal slice of the distal humerus TM 1517g (upper row; detail in the central row); (b) coronal slice of the proximal ulna TM 1517e (upper row; detail in the central row); and (c) transversal slice of the distal hallucial phalanx TM 1517k (upper row; detail in the central row). For comparison, the lower row shows the virtual slices of the distal humerus (a), the proximal ulna (b), and the distal hallucial phalanx (c) of a 16 year old male individual with traces of in progress diaphyseo-epiphyseal fusion. The white arrows indicate faint preserved traces of recent fusion in TM 1517e and TM 1517k. Scale bar, 1 cm

(Dean, Beynon, Thackeray, & Macho, 1993). While judging its frequency currently depends on random "snap-shot" radiographs taken on very small samples, this pattern may be more common in *Gorilla* than in *Pan* (Dean, 2010). Certainly because of incomplete preservation of the fossil record, but also due to still limited radiographic/microtomographic documentary material exploitable for comparisons, the combination M2 $A_{1/2}$-M3 $R_{1/2}$ seems also uncommon in fossil hominins. According to our review, the *Australopithecus africanus* TM (Sts) 1511, the *Paranthropus boisei* OH 5 and the *P. robustus* SK 13/14 specimens show a condition close to, while not fully overlapping, that of TM 1517 (see review in Supporting Information 2).

In humans, on average, the fusion of the distal hallucial phalanx slightly precedes that of the distal humerus (Cunningham et al., 2016). In gorillas, the distal humerus fuses earlier, followed by the proximal ulna and then by the toe phalanges (Randall, 1944), while in chimpanzees the diaphyseo-epiphyseal fusion sequence more commonly observed for these three bones is distal humerus—distal hallucial phalanx—proximal ulna (Brimacombe et al., 2015; Cameron et al., 2017). As already noted, while the signal in TM 1517 may be locally disturbed by the fading effects of fossilization, notably internally, the present evidence suggests a postcranial fusion sequence in this *P. robustus* individual closer to the great ape pattern.

As it is usually the case in the absence of direct information on enamel and dentine formation rates, assessing the most likely age at death interval in incomplete fossil specimens by crossing dental and postcranial evidence is a tentative, probabilistic exercise, which allows to assess the relative odonto-postcranial development of fossil individuals. In the case of TM 1517, this is especially true because its incomplete assemblage is so far the only representative of an immature *P. robustus* individual.

Judged against known age Virunga mountain gorillas at broadly the same stage of dental development, TM 1517 would fall between the ages of 10.69 and 14.94 years at the time of death (Boughner et al., 2012; Kralick et al., 2017) while, by assuming a *Gorilla*-like skeletal developmental model, TM 1517 would be younger than 8.5 years, if female, and between 9 and 12.5 years, if male (Leigh, 1992). When the *Pan* pattern is considered as a compatible model, TM 1517 would be 7.01–10.75 year old dentally (Boughner et al., 2012; Kuykendall & Conroy, 1996) and between 7.95 and 13.5 years old based on its skeletal maturation (Brimacombe et al., 2015, 2018; Cameron et al., 2017). By using extant human standards, the dental age at death of TM 1517 could be established between 11.65 and 15.25 years, based on the M2's stage of apex closure, and within the broader age interval 12.8–-19.91 years when the stage M3 $R_{½}$ is used (AlQahtani et al., 2010;

**TABLE 1** The maturational condition of the TM 1517 dental (following Moorrees et al., 1963) and postcranial elements (for the maturational stages, see Section 2.2) compared to the human and African great ape reference patterns

| TM 1517 condition | Age range[a] extant humans | Age range[a] great apes | Great ape versus human pattern | References[b] |
|---|---|---|---|---|
| LM2 stage $A_{1/2}$ | 11.65–15.08 (F)<br>14.78–15.25 (M) | *Gorilla*:<br>10.69–14.94 (M + F)<br>*Pan*:<br>7.01–10.75 (M + F) | – | Boughner, Dean, & Wilgenbusch, 2012; Kralick et al., 2017; Kuykendall & Conroy, 1996; Liversidge et al., 2006 |
| LM3 stage $R_{1/2}$ | 12.8–19.91 (M + F) | *Gorilla*:<br>10.69–12.71 (M + F)<br>*Pan*:<br>7.01–10.75 (M + F) | – | AlQahtani, Hector, & Liversidge, 2010; Boughner et al., 2012; Kralick et al., 2017; Kuykendall & Conroy, 1996 |
| Distal humerus:<br>Complete fusion | 13–15 (F)<br>16–19 (M) | *Gorilla*:<br><8.5 (F)<br>9–12.5 (M)<br>*Pan*:<br>7.95–13.5 (M + F) | – | Brimacombe, Kuykendall, & Nystrom, 2018; Cameron et al., 2017; Leigh, 1992 |
| Proximal ulna:<br>Fusion in progress<br>(not fully achieved) | 12–15 (F)<br>11–20 (M) | *Gorilla*:<br><8.5 (F)<br>9–12.5 (M)<br>*Pan*:<br>7.95–13.5 (M + F) | – | Brimacombe et al., 2018; Cameron et al., 2017; Leigh, 1992 |
| Distal hallucial phalanx:<br>Recently achieved<br>fusion | 11–16 (F)<br>14–18 (M) | *Gorilla*:<br><8.5 (F)<br><12.5 (M)<br>*Pan*:<br>9.45 (M + F) | – | Brimacombe, Kuykendall, & Nystrom, 2015; Cunningham et al., 2016; Leigh, 1992; Lordkipanidze et al., 2007; Paterson, 1929 |
| Fusion sequence:<br>1 = distal humerus<br>2 = dist. hall. phalanx<br>3 = proximal ulna | – | – | Great ape | Brimacombe et al., 2015; Cameron et al., 2017; Cunningham et al., 2016; Randall, 1944 |

Abbreviations: F, females, M, males.
[a]In years.
[b]See Supporting Information 3 for a full literature review.

Liversidge et al., 2006). In terms of human-based skeletal age, TM 1517 would have been between 11 and 16 years old if female, but would have fallen within the wider age interval of 11–20 years if male (see literature in Cunningham et al., 2016) (Supporting Information 3).

The three fossil hominin individual assemblages from Malapa (*Australopithecus sediba*), Dmanisi (*Homo erectus*), and Nariokotome (*H. erectus*) are of particular comparative interest here, since they associate postcranial elements to developing dentitions. Considering its combined dental and postcranial evidence, TM 1517 is developmentally older compared to all three such subadult individuals. Interestingly, a certain degree of disjunction between dental and skeletal maturational ages, the former indicating a distinctly earlier age at death, appears in both MH1 from Malapa (Cameron et al., 2017; Le Cabec, Tafforeau, Smith, Carlson, & Berger, 2014; Williams, Desilva, & De Ruiter, 2018) and KNM-WT 15000 from Nariokotome (Clegg & Aiello, 1999; Dean, 2016; Dean & Lucas, 2009; Dean & Smith, 2009; Smith, 1993) when a human maturational schedule is assumed as reference model, which is not the case when an ape pattern is considered (Supporting Information 4).

Sex is a further complicating factor when assessing maturational patterns in fossil hominins (Kaszycka, 2001). Indeed, for *P. robustus* it has been suggested that males experienced a slower and prolonged growth compared to the females to an extent compatible with a bimaturational growth pattern such as that of gorillas (Lockwood, Menter, Moggi-Cecchi, & Keyser, 2007) (Supporting Information 5). Accordingly, the still controversial assessment of the most likely sex identity of TM 1517 remains a limiting factor for elucidating the timing of its odonto-postcranial maturation process.

## ACKNOWLEDGMENTS

For access to fossil and comparative materials, we are grateful to the curatorial staff of the Ditsong National Museum of Natural History, Pretoria and the R. A. Dart Collection of the University of the Witwatersrand, Johannesburg. For the extant human comparative sample, ethical clearance was obtained from the Faculty of Health Sciences Research Ethics committee of the University of Pretoria (ref. no. 39/2016). We especially acknowledge N. Bacci (Johannesburg), B. Billing (Johannesburg), and L. Kgasi (Pretoria). We also thank L. Bam

(Pelindaba) and F. de Beer (Pelindaba) for analyses at Necsa. For scientific collaboration and generous availability to run independent measures for interobserver error assessment, we thank A. Beaudet (Johannesburg) and A. Mazurier (Poitiers). For data and information sharing, we thank P. Bayle (Bordeaux), J. Braga (Toulouse), B. Lans (Pretoria and Toulouse), and the Department of Human Evolution of the Max Planck Institute for Evolutionary Anthropology (Leipzig). For discussion, we thank E. L'Abbé (Pretoria), A. Beaudet, L. Bruxelles (Johannesburg and Toulouse), K. Carlson (Los Angeles and Johannesburg), F. E. Grine (Stony Brook), R. Hanon (Paris), D. Marchi (Pisa), E. Pouydebat (Paris), C. Theye (Pretoria), A. Val (Tübingen), B. Zipfel (Johannesburg). Finally, we are grateful to Trudy Turner, the Associate Editor, and two anonymous reviewers for constructive critique that considerably improved this manuscript. We acknowledge the DST-NRF for financial support (grant # UID23456) to establish the MIXRAD microfocus X-ray tomography facility at Necsa. M. C. was funded by the European Commission (EACEA), Erasmus Mundus programme, AESOP and AESOP + consortia (coord. by J. Braga), and by the Erasmus Mundus programme, Bakeng se Afrika and the NRF incentive grant associated with the NRF rated scientist A. C. Oettlé.

## DATA AVAILABILITY STATEMENT

The data that support the findings of this study are available from the corresponding author upon request and approval of the curatorial institutions.

## ORCID

*Marine Cazenave* https://orcid.org/0000-0001-7194-5958
*Clément Zanolli* https://orcid.org/0000-0002-5617-1613

## REFERENCES

Alemseged, Z., Spoor, F., Kimbel, W. H., Bobe, R., Geraads, D., Reed, D., & Wynn, J. G. (2006). A juvenile early hominin skeleton from Dikika, Ethiopia. *Nature*, *443*, 296–301.

AlQahtani, S. J., Hector, M. P., & Liversidge, H. M. (2010). Brief communication: The London atlas of human tooth development and eruption. *American Journal of Physical Anthropology*, *142*, 481–490.

Bolter, D. R., Elliott, M. C., Hawks, J., & Berger, L. R. (2020). Immature remains and the first partial skeleton of a juvenile *Homo naledi*, a late Middle Pleistocene hominin from South Africa. *PLoS One*, *15*, e0230440.

Boughner, J. C., Dean, M. C., & Wilgenbusch, C. S. (2012). Permanent tooth mineralization in bonobos (*Pan paniscus*) and chimpanzees (*P. troglodytes*). *American Journal of Physical Anthropology*, *149*, 560–571.

Braga, J., & Thackeray, J. F. (2016). *Kromdraai. A birthplace of Paranthropus in the Cradle of Humankind*. Stellenbosch, South Africa: Sun Press.

Brimacombe, C. S., Kuykendall, K. L., & Nystrom, P. (2015). Epiphyseal fusion in *Pan troglodytes* relative to dental age. *American Journal of Physical Anthropology*, *157*, 19–29.

Brimacombe, C. S., Kuykendall, K. L., & Nystrom, P. (2018). Epiphyseal fusion and dental development in *Pan paniscus* with comparisons with *Pan troglodytes*. *American Journal of Physical Anthropology*, *167*, 903–913.

Broom, R. (1938a). The Pleistocene anthropoid apes of South Africa. *Nature*, *142*, 377–379.

Broom, R. (1938b). Further evidence on the structure of the South African Pleistocene anthropoids. *Nature*, *142*, 897–899.

Broom, R. (1942). The hand of the ape-man, *Paranthropus robustus*. *Nature*, *149*, 513–514.

Broom, R., & Schepers, G. W. H. (1946). The South African fossil ape-men, the *Australopithecinae*. *Transvaal Museum Memoirs*, *2*, 18

Cameron, N., Bogin, B., Bolter, D., & Berger, L. R. (2017). The postcranial skeletal maturation of *Australopithecus sediba*. *American Journal of Physical Anthropology*, *163*, 633–640.

Cazenave, M., Oettlé, A., Thackeray, J. F., Nakatsukasa, M., de Beer, F., Hoffman, J., & Macchiarelli, R. (2019). The SKX 1084 hominin patella from Swartkrans Member 2, South Africa: An integrated analysis of its outer morphology and inner structure. *Comptes Rendus Palevol*, *18*, 223–235.

Choi, J. H., & Kim, C. Y. (1991). A study of correlation between the development of the third molar and second molar as an aid in age determination. *Journal of the Korean Academy of Oral Medicine*, *16*, 121–136.

Clegg, M., & Aiello, L. C. (1999). A comparison of the Nariokotome *Homo erectus* with juveniles from a modern human population. *American Journal of Physical Anthropology*, *110*, 81–93.

Cofran, Z., & Walker, C. S. (2017). Dental development in *Homo naledi*. *Biology Letters*, *13*, 20170339.

Cunningham, C., Scheuer, L., & Black, S. (2016). *Developmental juvenile osteology*. London, England: Academic Press.

Day, M. H., & Thornton, C. M. B. (1986). The extremity bones of *Paranthropus robustus* from Kromdraai B, East Formation Member 3, Republic of South Africa: A reappraisal. *Anthropos*, *23*, 91–99.

Dean, M. C. (2010). Retrieving chronological age from dental remains of early fossil hominins to reconstruct human growth in the past. *Philosophical Transactions of the Royal Society, London, Series B Biological Sciences*, *365*, 3397–3410.

Dean, M. C. (2016). Measures of maturation in early fossil hominins: Events at the first transition from australopiths to early *Homo*. *Philosophical Transactions of the Royal Society B: Biological Sciences*, *371*, 20150234.

Dean, M. C., Beynon, A. D., Thackeray, J. F., & Macho, G. A. (1993). Histological reconstruction of dental development and age at death of a juvenile *Paranthropus robustus* specimen, SK 63, from Swartkrans, South Africa. *American Journal of Physical Anthropology*, *91*, 401–419.

Dean, M. C., & Lucas, V. S. (2009). Dental and skeletal growth in early fossil hominins. *Annals of Human Biology*, *36*, 545–561.

Dean, M. C., & Smith, B. H. (2009). Growth and development of the Nariokotome youth, KNM-WT 15000. In F. E. Grine, J. G. Fleagle, & R. E. Leakey (Eds.), *The first humans. Origin and early evolution of the genus Homo* (pp. 101–120). New York, NY: Springer.

Dean, M. C., & Wood, B. A. (2003). A digital radiographic atlas of great apes skull and dentition. In L. Bondioli & R. Macchiarelli (Eds.), *Digital archives of human paleobiology*. (CD-ROM). Milano, Italy: ADS Solutions.

Kaszycka, K. A. (2001). A new graphic reconstruction of the type specimen of *Australopithecus robustus* from Kromdraai, South Africa-TM 1517. *South African Journal of Science*, *97*, 404–409.

Kelley, J., & Bolter, D. (2013). Growth, development, and life history in hominin evolution. In D. Begun (Ed.), *A companion to palaeoanthropology* (pp. 97–117). New York, NY: Wiley-Liss.

Kralick, A. E., Burgess, M. L., Glowacka, H., Arbenz-Smith, K., McGrath, K., Ruff, C. B., … McFarlin, S. C. (2017). A radiographic study or permanent molar development in wild Virunga mountain gorillas of known chronological age from Rwanda. *American Journal of Physical Anthropology*, *163*, 129–147.

Kuykendall, K. L., & Conroy, G. C. (1996). Permanent tooth calcification in chimpanzees (*Pan troglodytes*): Patterns and polymorphisms. *American Journal of Physical Anthropology*, *99*, 159–174.

Le Cabec, A., Tafforeau, P., Smith, T. M., Carlson, K., & Berger, L. (2014). Age-at-death and dental developmental pattern of the *Australopithecus sediba* juvenile MH1 determined from synchrotron virtual paleohistology. In *Proceedings of the 4th annual meeting of the European Society for the Study of Human Evolution* (Vol. 3, p. 103). Florence: European Society for the Study of Human Evolution (ESHE).

Leigh, S. R. (1992). Patterns of variation in the ontogeny of primate body size dimorphism. *Journal of Human Evolution*, *23*, 27–50.

Liversidge, H. M., Chaillet, N., Mornstad, H., Nystrom, M., Rowlings, K., Taylor, J., & Willems, G. (2006). Timing of Demirjian's tooth formation stages. *Annals of Human Biology*, *33*, 454–470.

Lockwood, C. A., Menter, C. G., Moggi-Cecchi, J., & Keyser, A. W. (2007). Extended male growth in a fossil hominin species. *Science*, *318*, 1443–1446.

Lordkipanidze, D., Jashashvili, T., Vekua, A., de León, M. S. P., Zollikofer, C. P., Rightmire, G. P., … Nioradze, M. (2007). Postcranial evidence from early *Homo* from Dmanisi, Georgia. *Nature*, *449*, 305–310.

Moorrees, C. F., Fanning, E. A., & Hunt, E. E., Jr. (1963). Age variation of formation stages for ten permanent teeth. *Journal of Dental Research*, *42*, 1490–1502.

Paterson, R. S. (1929). A radiological investigation of the epiphyses of the long bones. *Journal of Anatomy*, *64*, 28–46.

Randall, F. E. (1944). The skeletal and dental development and variability of the *Gorilla* (Concluded). *Human Biology*, *16*, 23–76.

Schwartz, G. T. (2012). Growth, development, and life history throughout the evolution of *Homo*. *Current Anthropology*, *53*, 395–408.

Schwartz, J. H., & Tattersall, I. (2005). *The human fossil record, craniodental morphology of early hominids (genera Australopithecus, Paranthropus, Orrorin), and overview* (Vol. 4). New York, NY: Wiley Liss.

Šešelj, M. (2017). Brief communication: An analysis of dental development in Pleistocene *Homo* using skeletal growth and chronological age. *American Journal of Physical Anthropology*, *163*, 531–541.

Skinner, M. F., & Sperber, G. H. (1982). *Atlas of radiographs of early man*. New York, NY: A. R. Liss.

Skinner, M. M., Kivell, T. L., Potze, S., & Hublin, J.-J. (2013). Micro-tomographic archive of fossil hominin specimens from Kromdraai B, South Africa. *Journal of Human Evolution*, *64*, 434–447.

Smith, B. H. (1993). The physiological age of KNM-WT 15000. In A. Walker & R. Leakey (Eds.), *The Nariokotome Homo erectus skeleton* (pp. 195–200). Cambridge, MA: Harvard University Press.

Smith, S. L. (2004). Skeletal age, dental age, and the maturation of KNM-WT 15000. *American Journal of Physical Anthropology*, *125*, 105–120.

Straus, W. L. (1948). The humerus of *Paranthropus robustus*. *American Journal of Physical Anthropology*, *6*, 285–313.

Thackeray, J. F., Braga, J., Sénégas, F., Gommery, D., Potze, S., & Senut, B. (2005). Discovery of a humerus shaft from Kromdraai B: Part of the skeleton of the type specimen of *Paranthropus robustus* Broom, 1938? *Annals of the Transvaal Museum*, *42*, 92–93.

Thackeray, J. F., De Ruiter, D. J., Berger, L. R., & Van Der Merwe, N. J. (2001). Hominid fossils from Kromdraai: A revised list of specimens discovered since 1938. *Annals of the Transvaal Museum*, *38*, 43–56.

Thackeray, J. F., McBride, V. A., Segonyane, S. P., & Franklyn, C. B. (2003). Trace element analysis of breccia associated with the type specimen of *Australopithecus* (*Paranthropus*) robustus from Kromdraai. *Annals of the Transvaal Museum*, *40*, 147–150.

Vekua, A., Lordkipanidze, D., Rightmire, G. P., Agusti, J., Ferring, R., Maisuradze, G., … Zollikofer, C. (2002). A new skull of early *Homo* from Dmanisi, Georgia. *Science*, *297*, 85–89.

Williams, S. A., DeSilva, J. M., & De Ruiter, D. J. (2018). Malapa at 10: Introduction to the special issue on *Australopithecus sediba*. *PaleoAnthropology*, *2018*, 49–55.

## SUPPORTING INFORMATION

Additional supporting information may be found online in the Supporting Information section at the end of this article.

**How to cite this article:** Cazenave M, Dean C, Zanolli C, et al. Reassessment of the TM 1517 odonto-postcranial assemblage from Kromdraai B, South Africa, and the maturational pattern of *Paranthropus robustus*. *Am J Phys Anthropol*. 2020;172: 714–722. https://doi.org/10.1002/ajpa.24082